

# New Physics in GaN Resonant Tunneling Diodes

Huili Grace Xing<sup>a,b,c,†</sup>, Jimmy Encomendero<sup>a</sup>, and Debdeep Jena<sup>a,b,c</sup>

<sup>a</sup>School of Electrical and Computer Engineering, Cornell University, Ithaca, New York, USA

<sup>b</sup>Department of Materials Science and Engineering, Cornell University, Ithaca, New York, USA

<sup>c</sup>Kavli Institute at Cornell for Nanoscale Science, Cornell University, Ithaca, New York, USA

## ABSTRACT

The outstanding material properties of III-Nitride semiconductors, has prompted intense research efforts in order to engineer resonant tunneling transport within this revolutionary family of wide-bandgap semiconductors. From resonant tunneling diode (RTD) oscillators to quantum cascade lasers (QCLs), III-Nitride heterostructures hold the promise for the realization of high-power ultra-fast sources of terahertz (THz) radiation. However, despite the considerable efforts over last two decades, it is only during the last three years that room temperature resonant tunneling transport has been demonstrated within the III-Nitride family of semiconductors.

In this paper we present an overview of our current understanding of resonant tunneling transport in polar heterostructures. In particular we focus on double-barrier III-Nitride RTDs which represents the simplest device in which the dramatic effects of the internal polarization fields can be studied. Tunneling transport within III-heterostructures is strongly influenced by the presence of the intense spontaneous and piezoelectric polarization fields which result from the non-centrosymmetric crystal structure of III-Nitride semiconductors. Advances in heterostructure design, epitaxial growth and device fabrication have led to the first unequivocal demonstration of robust and reliable negative differential conductance. which has been employed for the generation of microwave power from III-Nitride RTD oscillator. These significant advances allowed us to shed light into the physics of resonant tunneling transport in polar semiconductors which had remained hidden until now.

**Keywords:** Resonant Tunneling Diodes, III-Nitride Semiconductors, Resonant Tunneling Diode Oscillators, Resonant Tunneling Transport.

## 1. INTRODUCTION

Double-barrier resonant tunneling diodes (RTDs) represent the simplest device in which the physics of resonant tunneling transport can be studied in detail. Nitride-based resonant tunneling transport has been under scrutiny over the last two decades due to the unique optical and electronic material properties of III-Nitride heterostructures. Initial experiments employed a hetero-epitaxial growth approach to engineer resonant tunneling injection in III-Nitride RTDs.<sup>1-4</sup> However, this growth technique results in a high density of defects which act as electron traps, leading to self-charging effects and preventing coherent resonant tunneling transport. To reduce the number of defects per device, small-area RTDs have been recently designed, showing that repeatable negative differential conductance (NDC) can be achieved for RTDs grown on sapphire substrates, with a total wafer yield of  $\sim 45\%$ .<sup>5</sup>

The availability of single-crystal III-Nitride substrates enabled a significant reduction of the defect densities across the active region of polar III-Nitride RTDs, which led to the first observation of repeatable NDC at cryogenic temperatures.<sup>6,7</sup> The crystal high-quality of the homo-epitaxial growth can be seen in Fig. 2(a), which shows a transmission electron microscopy (TEM) image of the cross-section of the double-barrier active region of a typical GaN/AlN RTD, grown in our laboratory.<sup>8</sup> As a result of the, room-temperature current-voltage (I-V) measurements show clear regions of NDC across different heterostructure designs and with device areas up to  $400 \mu\text{m}^2$ . As a result of robust tunneling transport exhibited by our devices, we have been able to identify several unique features in the tunneling spectrum which are intimately linked with the strong polarization fields present in III-Nitride semiconductors.<sup>8</sup> In this paper we discuss the novel tunneling features exhibited by III-Nitride

<sup>†</sup>E-mail: grace.xing@cornell.edu

RTDs which have been also generalized for the entire class of polar RTDs. Finally, the robust NDC exhibited by our devices is employed for the design of the first III-Nitride RTD oscillators showing that active sources of radiation can be designed employing this long-sought quantum devices.<sup>9</sup>

## 2. RESONANT TUNNELING PHYSICS IN POLAR RTDS

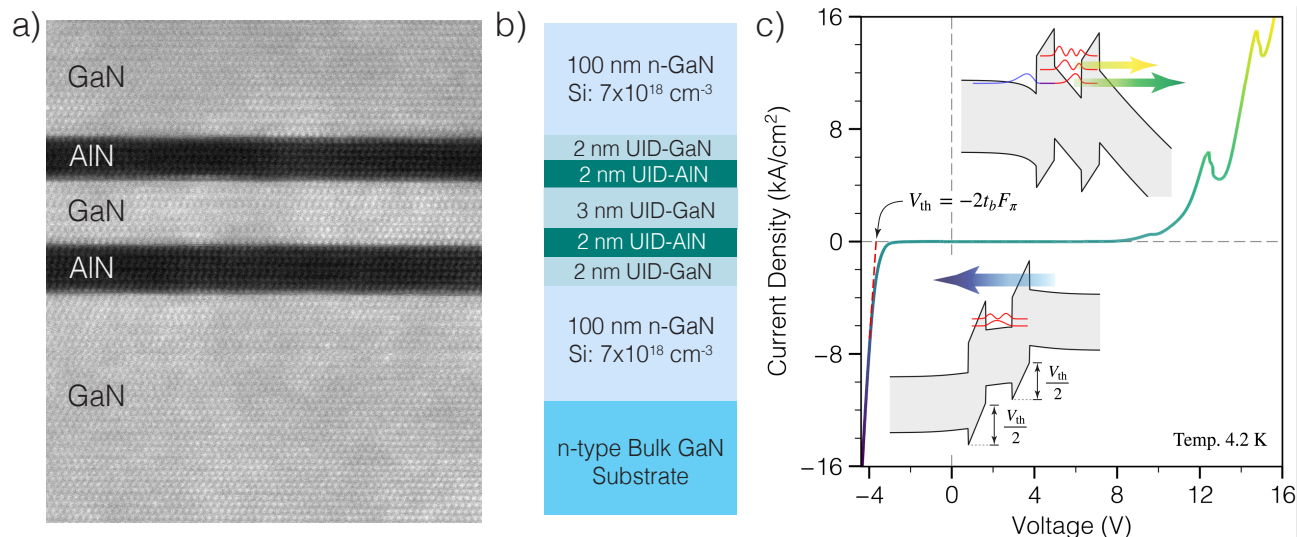


Figure 1. GaN/AlN Resonant Tunneling Diode. a) High-resolution Transmission electron microscopy (TEM) image of double-barrier active region showing the high-quality of the homo-epitaxial growth. b) Schematic of a III-Nitride RTD grown by MBE, showing the typical doping levels in the collector and emitter contacts. c) Current-voltage characteristics of the RTD device depicted in Fig. 2(b), measured at a temperature of 4.2 K.

The non-centrosymmetric crystal structure of III-Nitride semiconductors gives rise to intense spontaneous and piezoelectric polarization fields which dramatically influence vertical transport across the double-barrier active region. These strong polarization fields have been harnessed in various electronic and photonic devices to assist in p-type doping,<sup>10</sup> enhance Zener interband tunneling<sup>11</sup> and induce a highly conductive 2D electron gas (2DEG).<sup>12</sup> However, tunneling injection, being exponentially sensitive to the internal electric fields and potential barriers, stands as unique phenomenon to understand the influence exerted by the internal polarization fields on the resonant tunneling dynamics.<sup>13</sup>

Figure 1(b) shows the schematic cross-section of a typical double-barrier GaN/AlN resonant tunneling diode. Molecular beam epitaxy (MBE) was employed to grow the device structure atop a single-crystal n-type GaN substrate. Reflection high-energy electron diffraction (RHEED) was monitored during the epitaxial process to achieve real-time control over the number of monolayers incorporated into the device structure.<sup>13</sup> Further Details on the epitaxial growth, control over the thickness of the tunneling barriers, structural characterization and diode fabrication process can be found elsewhere.<sup>8,13</sup>

Figure 1(c) shows the typical cryogenic current-voltage ( $I$ - $V$ ) characteristics of the RTD shown schematically in Fig. 1(b). The effect of the tunneling barriers can be seen clearly under low voltage bias, which results in the blocking of the tunneling carries across the active region. Under relatively high voltage bias ( $V_{\text{bias}} > 8$  V), the resonant tunneling levels get aligned with the emitter electrons, leading to an enhancement in the magnitude of the resonant tunneling current, as can be seen from Fig.1 (c). The peak in the  $I$ - $V$  curve corresponds to the resonant alignment between the ground-state and the emitter subband present in the accumulation region [see top inset of Fig. 1(c)]. When the biased is increased further, the de-tuning between the energies of the ground-state and the accumulation subband leads to the clear NDC region. For even larger voltage bias, the first-excited state of the quantum well is also brought into resonance with the emitter region. This resonant level supports an injection current of  $\sim 15.5$  kA/cm<sup>2</sup> right at the resonant condition.

Current injection under reverse bias does not exhibit the strong conductance modulation that was measured in forward direction. In contrast, current levels of the order of  $\sim 15.5 \text{ kA/cm}^2$  can be attained with a much lower reverse bias (i.e.  $V_{\text{bias}} \approx -4.1 \text{ V}$ ). This asymmetry in current injection is a direct consequence of the internal polarization of the double-barrier active region. As can be seen in the bottom inset of Fig. 1(c), under reverse bias, the emitter barrier experiences a strong modulation as a result of the depopulation of the 2DEG next to it. As a result, carriers injected from the collector side tunnel only across the collector barrier [indicated by the blue arrow in Fig. 2(c)]. A critical voltage is reached when the 2DEG is completely depopulated and the electric fields across the tunneling barriers originate only from the internal polarization charges at the GaN/AlN interfaces ( $\sigma_\pi$ ). This critical condition corresponds to the band diagram shown in the bottom inset of Fig. 1(c). Since only the AlN barriers support the overall internal polarization field ( $F_\pi = e\sigma_\pi/\epsilon_s$ , where  $e$  is the electron charge and  $\epsilon_s$  is the GaN dielectric constant), the critical threshold voltage can be expressed by the simple relationship:<sup>8</sup>

$$V_{\text{th}} = -2t_b F_\pi \quad (1)$$

Equation (1) can be employed to experimentally measure the magnitude of the internal polarization fields ( $F_\pi$ ). To do so we can employ a set of GaN/AlN RTDs with different barrier thickness ( $t_b$ ). After measuring their critical threshold voltage ( $V_{\text{th}}$ ), we can see that the slope of the  $V_{\text{th}}$ -vs.- $t_b$  plot will be given by twice the magnitude of the internal built-in polarization fields.<sup>8</sup>

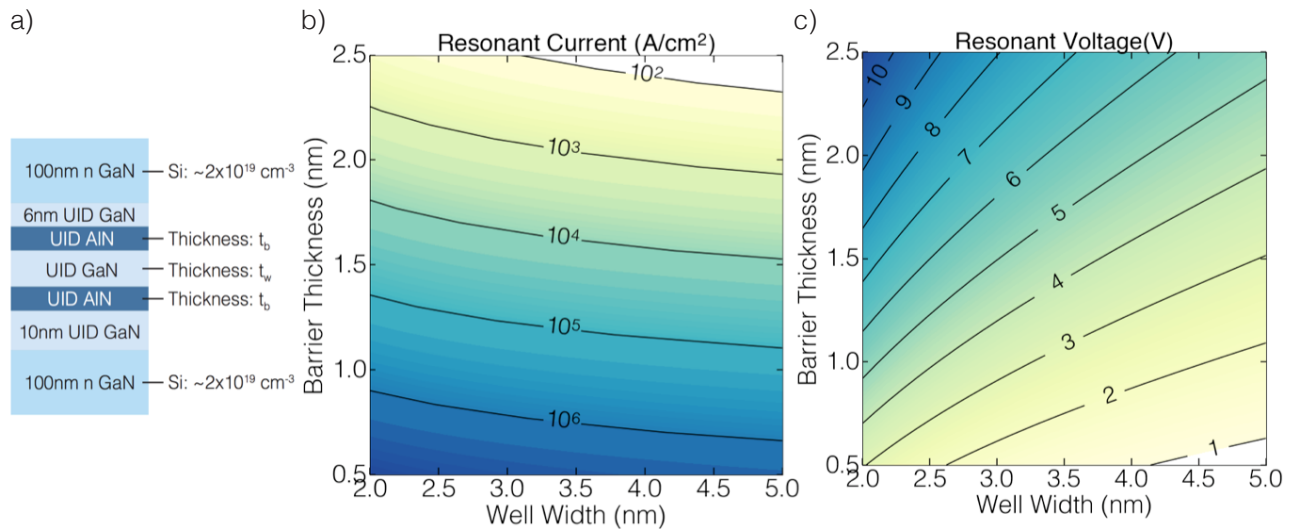


Figure 2. Design space of a general GaN/AlN RTD. a) Schematic cross-section of GaN/AlN RTD with variable barrier and quantum well thicknesses ( $t_b$  and  $t_w$ , respectively). b) Theoretical resonant tunneling current calculated employing our analytical quantum transport model. c) Theoretical resonant tunneling voltage calculated employing the same quantum transport model.

### 3. QUANTUM TRANSPORT MODEL FOR POLAR RTDS

Engineering resonant tunneling injection in III-Nitride heterostructures presents some unique challenges due to the presence of the internal polarization fields. As we saw in the previous section, the intensity of these built-in polarization fields dramatically influences the tunneling transport regimes. To understand the main consequences of these internal fields, we have developed an analytical quantum transport model which completely captures its effects. This model, based on the Landauer-Büttiker quantum transmission approach, can be used to calculate the current-voltage characteristics of general polar-RTD.<sup>13</sup>

It should be noted that both the peak resonant voltage and the magnitude of the peak resonant tunneling current also exhibit a strong influence by the magnitude of  $F_\pi$ . These two parameters, being crucial for the design of RTD-oscillators, can be calculated employing our RTD model valid for the entire class of polar RTDs.<sup>8,13</sup>

Figure 2(a) shows the schematic cross-section of a GaN/AlN RTD in which we consider the thickness of the barriers ( $t_b$ ), and the thickness of the well ( $t_w$ ) as independent variables. Employing our model we have computed the expected resonant tunneling current, as can be seen in Fig. 2(b). It can be seen that the thickness of the tunneling barriers exert an exponential control of the magnitude of the peak current, as expected. Furthermore, since the tunneling barriers sustain a finite electric field even at zero bias, the equilibrium energy of the resonant states depends on the barrier thickness  $t_b$ . Consequently, the resonant voltage will depend on  $t_b$ , and on the magnitude of the polarization fields. Figure 2(c) shows the calculated value of the resonant voltage as a function of both the barrier thickness and width of the GaN quantum well. This novel transport theory allows us to completely explore the design space of polar III-Nitride RTDs as can be seen from Figs. 2(b) and (c).

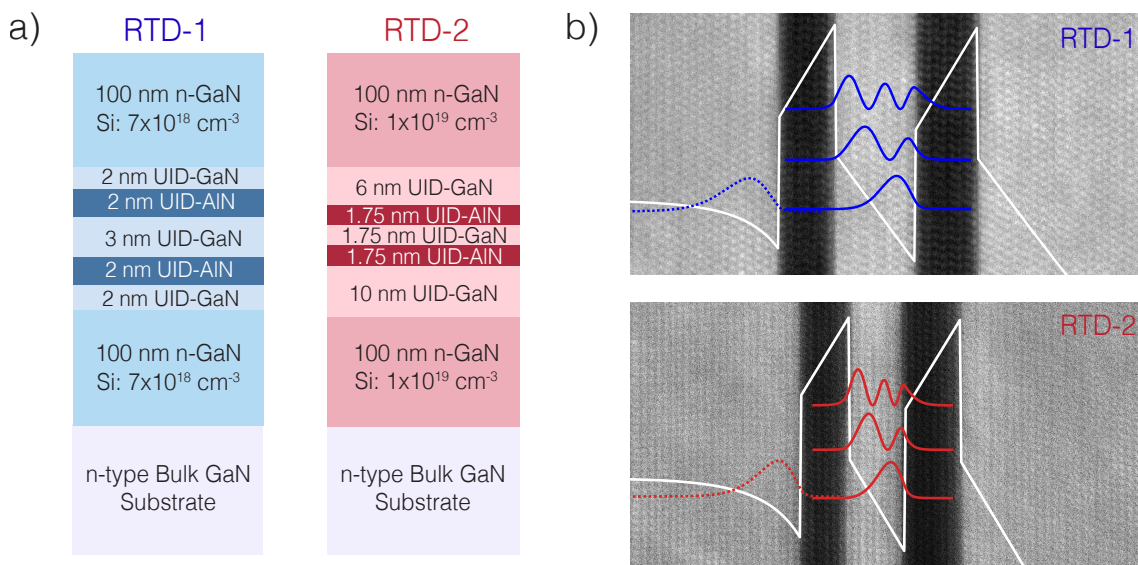


Figure 3. GaN/AlN Resonant Diodes with different peak currents. a) Schematic cross section of the device structure of two GaN/AlN RTD employed as active elements in III-Nitride RTD oscillators. b) High angle annular dark-field (HAADF) scanning transmission electron microscopy (STEM) images of each of the RTDs active regions. The overlay shows the conduction band profile as well as the confined quantum states.

#### 4. GAN/ALN RESONANT TUNNELING DIODE OSCILLATORS

Resonant tunneling diodes offer the possibility of tuning the electron transport dynamics, enabling ultra-fast carrier injection across the double-barrier active region. This important feature has been employed over the last decades to engineer arsenide-based RTDs with extremely high-current densities,<sup>14, 15</sup> leading to sub-picosecond tunneling times.<sup>16</sup> Attaining similar current levels is still one of the challenges for nitride-based RTDs. However, last year we demonstrated the first high-current density GaN/AlN RTD which was employed for the generation of microwave power; constituting the first practical application of nitride-based resonant tunneling injection.<sup>9</sup> This milestone, in conjunction with the demonstration of high tunneling current densities, show the great potential of these devices for the realization of high-power ultra-fast electronic oscillators.

Room temperature electrical oscillations have been studied in two different RTD designs which are schematically shown in Fig. 3(a). The main differences between these diodes are the quantum well width, barrier thickness, and the extension of the spacer regions next to each of the tunneling barriers. The incorporation of the desired number of monolayers in the barriers and quantum well was confirmed using high angle annular dark-field (HAADF) scanning transmission electron microscopy (STEM), as can be seen in Fig. 3(b). The overlays show the band diagrams at the resonant tunneling condition in which the ground-state aligns with the emitter subband.

Figure 4(a) shows the current-voltage characteristics of each RTD depicted in Fig. 3(a), measured at room temperature. Both RTDs present a characteristic resonant tunneling peak, driving  $\sim 180$  and  $\sim 6.4$  kA/cm<sup>2</sup>, respectively. The RTD-microwave oscillators were assembled by connecting the RTDs to a spectrum analyzer using a bias tee and coaxial cables.<sup>9</sup> When the devices are biased within the NDC region, self-oscillations are generated in biasing circuit. The output power spectrum of each oscillator is displayed in Fig 4(b), showing that a maximum frequency of oscillation of 0.94 GHz is produced by the high-current density RTD, generating 3.0 W of output power. Using an equivalent RTD circuit model, it is shown that the oscillation frequency is limited by the time constant of the external circuit instead of the tunneling time of the RTDs.<sup>9</sup> These results show the great potential of III-Nitride RTDs for the realization of high-frequency electronic oscillators.

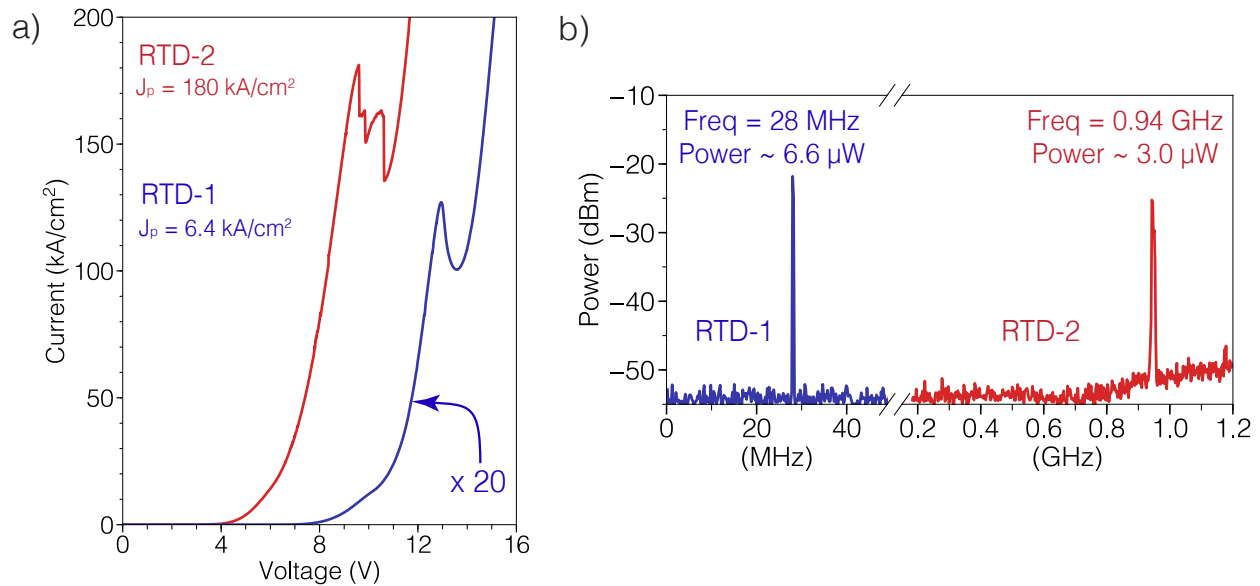


Figure 4. III-Nitride resonant tunneling diode oscillators. a) Room temperature current-voltage characteristics of the GaN/AlN RTDs shown in Fig. 3(a). The measured peak current densities are  $\sim 180$  kA/cm<sup>2</sup> and  $\sim 6.4$  kA/cm<sup>2</sup>. b) Power spectral density emitted by each of the III-Nitride RTD oscillators.

## 5. CONCLUSIONS

In conclusion, the recent advances in heterostructure design, epitaxial growth and device fabrication have led to a considerable improvement in the resonant tunneling performance of state-of-the-art III-Nitride resonant tunneling diodes. These findings represent important steps towards the understanding of resonant tunneling physics across polar heterostructures. Furthermore, the realization of the first RTD oscillators driven by GaN/AlN RTDs, show the great potential of these devices for the realization of high-power ultra-fast electronic oscillators. The new insights presented here pave the way for attaining the full potential of III-Nitride-based resonant tunneling devices in the near future.

## ACKNOWLEDGMENTS

This work was funded by the Office of Naval Research under the DATE MURI Program (Contract: N00014-11-10721, Program Manager: Dr. Paul Maki) and the National Science Foundation (NSF) MRSEC program (DMR-1719875). The authors also acknowledge partial support from NSF-DMREF (DMR-1534303) and EFRI-NewLAW (EFMA-1741694) programs. This work was performed in part at Cornell NanoScale Facility, an NNCI member supported by NSF Grant NNCI-1542081, and Cornell Center for Materials Research Shared Facilities which are supported through the NSF MRSEC program (DMR-1719875).



## REFERENCES

- [1] Kikuchi, A., Bannai, R., and Kishino, K., “AlGa<sub>N</sub> Resonant Tunneling Diodes Grown by rf-MBE,” *physica status solidi (a)* **188**(1), 187–190 (2001).
- [2] Foxon, C. T., Novikov, S. V., Belyaev, A. E., Zhao, L. X., Makarovskiy, O., Walker, D. J., Eaves, L., Dykeman, R. I., Danylyuk, S. V., Vitusevich, S. A., Kappers, M. J., Barnard, J. S., and Humphreys, C. J., “Current-voltage instabilities in GaN/AlGa<sub>N</sub> resonant tunnelling structures,” *physica status solidi (c)* **0**(7), 2389–2392 (2003).
- [3] Leconte, S., Golka, S., Pozzovivo, G., Strasser, G., Remmele, T., Albrecht, M., and Monroy, E., “Bi-stable behaviour in gan-based resonant tunnelling diode structures,” *physica status solidi c* **5**(2), 431–434 (2008).
- [4] Boucherit, M., Soltani, A., Monroy, E., Rousseau, M., Deresmes, D., Berthe, M., Durand, C., and De Jaeger, J.-C., “Investigation of the negative differential resistance reproducibility in AlN/GaN double-barrier resonant tunnelling diodes,” *Applied Physics Letters* **99**(18), 182109 (2011).
- [5] Wang, D., Su, J., Chen, Z., Wang, T., Yang, L., Sheng, B., Lin, S., Rong, X., Wang, P., Shi, X., Tan, W., Zhang, J., Ge, W., Shen, B., Liu, Y., and Wang, X., “Repeatable Room Temperature Negative Differential Resistance in AlN/GaN Resonant Tunneling Diodes Grown on Sapphire,” *Advanced Electronic Materials* **2018**, 1800651.
- [6] Li, D., Tang, L., Edmunds, C., Shao, J., Gardner, G., Manfra, M. J., and Malis, O., “Repeatable low-temperature negative-differential resistance from Al<sub>0.18</sub>Ga<sub>0.82</sub>N/gan resonant tunneling diodes grown by molecular-beam epitaxy on free-standing gan substrates,” *Applied Physics Letters* **100**(25), 252105 (2012).
- [7] Li, D., Shao, J., Tang, L., Edmunds, C., Gardner, G., Manfra, M. J., and Malis, O., “Temperature-dependence of negative differential resistance in gan/algan resonant tunneling structures,” *Semicond. Sci. Technol.* **28**(7), 074024 (2013).
- [8] Encomendero, J., Faria, F. A., Islam, S. M., Protasenko, V., Rouvimov, S., Sensale-Rodriguez, B., Fay, P., Jena, D., and Xing, H. G., “New tunneling features in polar III-Nitride resonant tunneling diodes,” *Physical Review X* **7**, 041017 (2017).
- [9] Encomendero, J., Yan, R., Verma, A., Islam, S. M., Protasenko, V., Rouvimov, S., Fay, P., Jena, D., and Xing, H. G., “Room temperature microwave oscillations in GaN/AlN resonant tunneling diodes with peak current densities up to 220 kA/cm<sup>2</sup>,” *Applied Physics Letters* **112**(10), 103101 (2018).
- [10] Simon, J., Protasenko, V., Lian, C., Xing, H., and Jena, D., “Polarization-induced hole doping in wide-band-gap uniaxial semiconductor heterostructures,” *Science* **327**(5961), 60–64 (2010).
- [11] Simon, J., Zhang, Z., Goodman, K., Xing, H., Kosel, T., Fay, P., and Jena, D., “Polarization-induced zener tunnel junctions in wide-band-gap heterostructures,” *Physical Review Letters* **103**, 026801 (Jul 2009).
- [12] Khan, M. A., Kuznia, J. N., Van Hove, J. M., Pan, N., and Carter, J., “Observation of a twodimensional electron gas in low pressure metalorganic chemical vapor deposited GaNAl<sub>x</sub>Ga<sub>1-x</sub>N heterojunctions,” *Applied Physics Letters* **60**(24), 3027–3029 (1992).
- [13] Encomendero, J., Protasenko, V., Sensale-Rodriguez, B., Fay, P., Rana, F., Jena, D., and Xing, H. G., “Broken symmetry effects due to polarization on resonant tunneling transport in double-barrier nitride heterostructures,” *Currently under review* (2019).
- [14] Izumi, R., Suzuki, S., and Asada, M., “1.98 THz resonant-tunneling-diode oscillator with reduced conduction loss by thick antenna electrode,” in [42nd International Conference on Infrared, Millimeter, and Terahertz Waves (IRMMW-THz)], 1–2 (Aug 2017).
- [15] Kanaya, H., Sogabe, R., Maekawa, T., Suzuki, S., and Asada, M., “Fundamental Oscillation up to 1.42 THz in Resonant Tunneling Diodes by Optimized Collector Spacer Thickness,” *Journal of Infrared, Millimeter, and Terahertz Waves* **35**, 425–431 (May 2014).
- [16] Kanaya, H., Maekawa, T., Suzuki, S., and Asada, M., “Structure dependence of oscillation characteristics of resonant-tunneling-diode terahertz oscillators associated with intrinsic and extrinsic delay times,” *Jpn. J. Appl. Phys.* **54**(9), 094103 (2015).